Detection of exciton polaritons in organic thin film TES-ADT

David Haas

An undergraduate thesis advised by Oksana Ostroverkhova

submitted to

Department of Physics, Oregon State University

In partial fulfillment of

the requirements for the degree of

Baccalaureate of Science in Physics

Presented May 10, 2019

Revised and resubmitted May 31, 2019

Abstract

Exciton polaritons are quasiparticles composed of a quantum superposition of matter and light states that arises from the coupling of a standing wave photon and an exciton. These quasiparticles show promise in the development of future technologies, such as polariton lasers, optical communication lines, solid state lighting, and medicine. This research has two primary objectives: to design and fabricate a Fabry-Perot microcavity system in which to produce exciton polaritons; and to show evidence of polariton occurrence by determining the Rabi splitting energy with angle resolved photoluminescence. The organic semiconductor anthradithiophene (ADT) incorporated in a host polymer PMMA matrix is the material of choice for this project. To construct the microcavities, we used e-beam deposition to coat a glass slide with silver, then spin cast a thin film of PMMA mixed with dilute anthradithiophene on top (ADT molecule spacing d), and then added a final layer of silver to complete the mirror chamber (cavity size L). By adjusting PMMA concentration and spin cast RPMs, we designed a process to produce a microcavity of just the right thickness to contain a standing wave photon whose energy is roughly equal to the exciton energy, about 2.37 eV. The relation between film thickness and PMMA concentration was established. To find the Rabi splitting energy, we excited the sample with a 355 nm laser, observed the photoluminescence emissions at varying angles of detection, and used the energies to find the dispersion relation with which the Rabi energy can be calculated. Rabi energies were calculated using photoluminescence data from two cavities at two laser polarizations for each. The Rabi energies from cavity 1B (L = 147 nm, d = 5 nm) were ~55 meV at s-polarization and p-polarization. The Rabi energies from cavity 1C (L = 149 nm, d = 4 nm) were ~61 meV for s-polarization, and ~31 meV for p-polarization. These energies are small as expected because the ADT is very dilute.

TABLE OF CONTENTS

LIST OF FIGURES

1 INTRODUCTION

1.1 MOTIVATION AND OBJECTIVE

Exciton polaritons are quasiparticles produced by a coupling of matter and light states to produce a quantum mechanical superposition that exhibits properties of both. These quasiparticles have been observed to occur naturally in some crystals and can be produced very efficiently in a Fabry-Perot microcavity [1]. Exciton polaritons are a recent fascination in experimental physics and have been used to achieve formation of Bose-Einstein condensates and superfluidity. The application of these quasiparticles in future tech development, such as polariton lasers, solid state lighting, optical communication lines, and medicine is highly anticipated [2]. Extensive study has been done regarding production of exciton polaritons within inorganic semiconductors, but this usually requires that the materials be kept at very low temperatures. Using organic semiconductors instead has many great benefits, such as low cost, convenient production by liquid deposition of thin films on flexible substrates, and strong photon-matter interaction at room temperature. Much more research is needed to discover the full utility and effectiveness of using these types of materials.

This research is intended to inform future research on the polaritonic behavior of crystalline anthradithiophene by first examining that of its simpler and better understood dilute form. My research has two primary objectives: to design and fabricate a Fabry-Perot microcavity system in which to produce exciton polaritons; and to show evidence of polariton occurrence by determining the Rabi splitting energy with angle resolved photoluminescence.

1.2 EXCITON POLARITON QUASI-PARTICLES

Polaritons can form from the result of the coupling of light with several types of oscillating electric dipoles, such as excitons, phonons, and plasmons. This paper discusses exciton-

polaritons which arise from strong coupling of excitons and photons. When a photon is absorbed by the semiconductor molecule, an exciton (an electron-hole pair) is created by bumping an electron to a higher energy state. After a short time, the electron-hole pair will collapse, emitting a photon of the same energy as the original excitation. This photon then becomes a standing wave in the cavity to be reabsorbed by the semiconductor molecule. By containing this process inside of an optical resonance microcavity and pumping it with a laser, these exciton-photon oscillations will occur in a cyclical manner.

Exciton-polaritons are called quasi-particles because their behavior can be modeled like particles, but this behavior arises not from a single object, but from a collective of particles and interactions. As quasiparticles, exciton-polaritons gain interesting properties from their photon and exciton constituents. They have large cross-section interactions and spin, like an exciton, and they have very small mass, can be measured optically, and follow boson statistics like a photon [3]. In order for an exciton-polariton to form, the exciton must be in resonance with the cavity photon in a consistent cycle of excitation and decay, and their "rate of energy exchange [must be] faster than the decay rates of both constituents" [3].

1.3 MICROCAVITIES

Microcavities are commonly employed in polaritonics research as a means to trap excitons and photons together. A Fabry-Perot microcavity, or optical resonance cavity, is a very thin chamber, typically measuring in nanometers or micrometers, of two opposing mirrors that can house a standing wave of light. By carefully designing the dimensions of the cavity, one can select the frequency of light that is allowed to persist as a standing wave, or optical mode. This is known as the cavity's resonance frequency. In order for a cavity to support a standing wave photon, the cavity thickness must be some integer multiple of half of the photon's wavelength.

However, the wavelength of the cavity photon will be dependent on the cavity's effective index of refraction.

One of the goals of this project is to create cavities that can contain a standing wave photon whose energy is a little less than the exciton energy (about 2.37 eV). Using the equation

$$E = \frac{hc}{\lambda} = \frac{1240}{\lambda}, \quad (1)$$

with E being the energy of the photon in eV and λ being the photon's wavelength in nm, we can determine that a photon of 2.37 eV would have a wavelength of ~523 nm in a vacuum. However, the PMMA inside the cavity has a refractive index of n = 1.49, shortening the photon wavelength to ~341 nm, which calls for a cavity size of ~170.5 nm to house a half wavelength. The effective index of refraction, which is easily measured by ellipsometry, is a bit different due a few factors. The amount of ADT (n ~1.8) in the cavities is small enough that we considered it to be negligible. The effective index of a material is also dependent on wavelength, because of dispersion, and to laser polarization, because of the polarizability of the material.

The concentration of ADT in these cavities will be so low that it becomes useful to describe it in terms of the average distance between molecules, d. This distance can be obtained by

$$V = \frac{4\pi}{3}\left(\frac{d}{2}\right)^3, \quad (2)$$

where *V* is the volume per molecule and *d* is distance between guest molecules (ADT in this case). And then,

$$\mathrm{d} = 2\sqrt[3]{\frac{3V}{4\pi}}, \quad (3)$$

and after some derivation,

$$\mathrm{d} = 2\sqrt[3]{\frac{3\,M_H\,f}{4\,\pi\,\rho_H}}, \tag{4}$$

where M_H and ρ_H are the monomer molar mass and density of the host molecule (PMMA), and f is the mole ratio,

$$f = \frac{mols\ of\ host\ (PMMA)}{mols\ of\ guest\ (ADT)}, \tag{5}$$

which changes Equation (3) to,

$$d = 0.644\ \mathrm{nm}\ \sqrt[3]{f}. \tag{6}$$

1.4 RABI SPLITTING

Typically, the coupling between photons and excitons is quite weak, but inside a microcavity that is tuned near the resonance of the exciton emission, the photon and exciton can enter the strong coupling regime. Strong coupling is said to occur (in the context of paramagnetic systems) when the Rabi energy is significant enough to be experimentally observed [4]. So, what is the Rabi energy and how is it determined? Using a coupled harmonic oscillator model, we can imagine a single photon and exciton system represented by the equation,

$$\begin{bmatrix} E_p & V \\ V & E_x \end{bmatrix} \begin{bmatrix} \alpha \\ \beta \end{bmatrix} = \mathrm{E} \begin{bmatrix} \alpha \\ \beta \end{bmatrix}, \tag{7}$$

where E_p is the energy of the uncoupled photon, E_x is the energy of the uncoupled exciton, V is the interaction potential, and α and β are eigenvector mixing coefficients [5]. The coupling causes a splitting in energy, 2V, when E_p and E_x are equal (Figure 1)

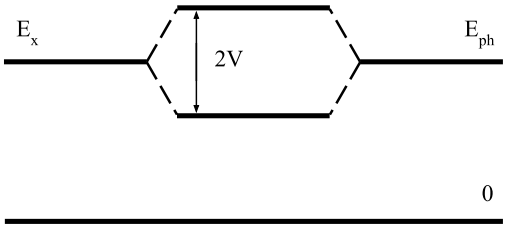

Figure 1 In the coupled system, the exciton and photon become indistinguishable and energy splitting occurs. The energy difference between the upper and lower polariton energies is the Rabi energy.

Equation (7) leads to the eigen values,

$$E_{\pm}(\theta) = \frac{E_x + E_{ph}(\theta)}{2} \pm \sqrt{V^2 + \left(\frac{E_x + E_{ph}(\theta)}{2}\right)^2}, \tag{8}$$

where E_x (~2.37 eV) is the exciton energy, $2V$ is the Rabi energy, E_{ph} is the photon energy as defined in,

$$E_{ph}(\theta) = E_{ph}^0 \left(1 - \frac{\sin^2(\theta)}{(n_{eff})^2}\right)^{-1/2}, \tag{9}$$

with E_{ph}^0 as the photon energy at normal incidence, θ as the angle of detection, and n_{eff} as the effective index of refraction as measured by ellipsometry. Equation (8) gives the dispersion relation shown in Figure 2, where the anti-crossing occurs when E_p and E_x are equal. These equations can be generalized to a system with many photons and excitons.

For some perspective, the first evidence of polaritonic behavior in an organic system was a spun cast film of tetra-(2,6-t-butyl)phenol-porphyrin zinc (4TBPPZn) in polystyrene tested by Lidzey et al. at room temperature and yielded a Rabi splitting of >100 meV.

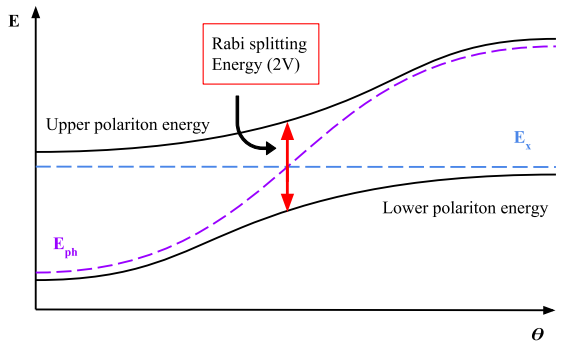

Figure 2 Demonstration of the energies of the exciton, photon, and polariton over a range of angles of reflectance. The exciton energy (E_x), when isolated, is independent of θ. The photon energy (E_{ph}), when isolated, varies with the angle of emission, θ. When coupled, the exciton and photon exchange energy and anti-crossing occurs. The difference in coupled energies (2V) is the Rabi energy.

1.5 TES-ADT PROPERTIES

To explore the use of organic semiconductors in polaritonics, this project uses a molecule that is technically labeled, dif-TES-ADT (2,8-Difluoro-5,11-bis(triethylsilylethynyl)anthradithiophene, hereafter referred to as anthradithiophene, or simply ADT (Figure 3). This molecule was chosen because of its ability to house delocalized electrons along its backbone of conjugated double bonds, its high charge carrier mobility (~7 cm^2/Vs), and because of its long-lived excited state (>10 ns), which is important for the generation of exciton-polaritons. Various substitutions on the molecule can be introduced which enables tunability of properties.

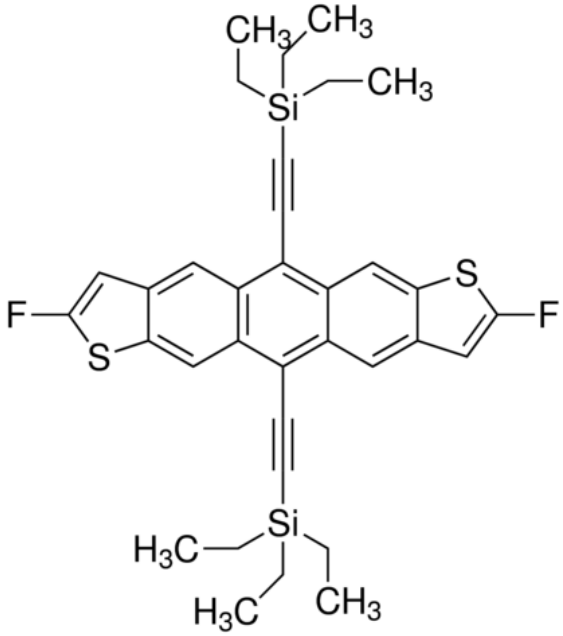

Figure 3 Molecular structure of dif-TES-ADT. Organic semiconductor Anthradithiophene (ADT) molecule. This molecule was selected because of its ability to house delocalized electrons along its backbone of conjugated double bonds and its long-lived excited state (>10 ns).

Because the optical and electrical properties of ADT are largely determined by its backbone structure, changing ADT's side groups will not alter its ability to produce polaritonic states. By switching the side groups, we can change the way the ADT molecules stack together when in crystalline form, which will determine what kind of excitons are allowed or encouraged in the crystal. For now, we will use dilute ADT to isolate the individual molecules and limit complicated interactions.

2 METHODS

2.1 CAVITY DESIGN

The first step was to engineer a process of creating microcavities of any desired thickness. A stock solution was made for spin casting by mixing Polymethylmethacrylate (PMMA) powder with toluene and sonicating with heat for 20 minutes. The stock solution was made to be 1 mol/L using 100 g/mol for PMMA (monomer) stoichiometry calculations. The solution was diluted several times to be spin cast onto six silver coated glass slides (100 nm Ag) at PMMA concentrations of 0.1 M, 0.3 M, 0.4 M, 0.5 M, 0.7 M, and 1.0 M. Several concentrations were tested to understand the relationship between processing conditions and thickness. All spin casting was performed using 100 µL solution at 1000 RPM for 40 seconds.

PMMA powder was obtained from Aldrich Chemistry (item # 200336-50G) with refractive index n = 1.49. Powder mass was measured with Sartorius GD603 balance. Toluene was obtained from J. T. Baker company (item # 9351-02). Toluene and stock solutions were measured with µL precision pipettes. Sonication of initial stock solution was done with a 1510 Branson sonicator. Thin films were deposited with Laurell spin caster, model WS-400BZ-6NPP/LITE.

PMMA thickness measured with ellipsometer. The ellipsometer machine was fed information about the composition of each layer and a guess at expected values for refractive index and thicknesses. The ellipsometer was then able to use a Lorentz dielectric model to calculate experimental values. A profilometer was used first to calculate film thickness, but the stylus that the profilometer uses to determine the profile of the sample does so with physical contact and was deforming the sample slides and producing unreliable results.

Possible sources of error in cavity design include solution evaporation during brief periods when vial was open, solution lost to residue on pipette tips, and possible rounding error during stoichiometry calculations (four significant figures were kept).

The project lead, Jonathan Van Schenck, created a series of thin film slides containing various concentrations of ADT as the next step in the engineering process to create the perfect microcavity for hosting exciton polaritons. These slides were composed of a bottom layer of silver (100 nm), a film of different ADT:PMMA blends (thicknesses ranging from 139.6 nm to 144 nm), and a thin top coat of silver (30 nm) that resembles a grid of dots, each about 5 mm in diameter, as depicted in Figure 4.

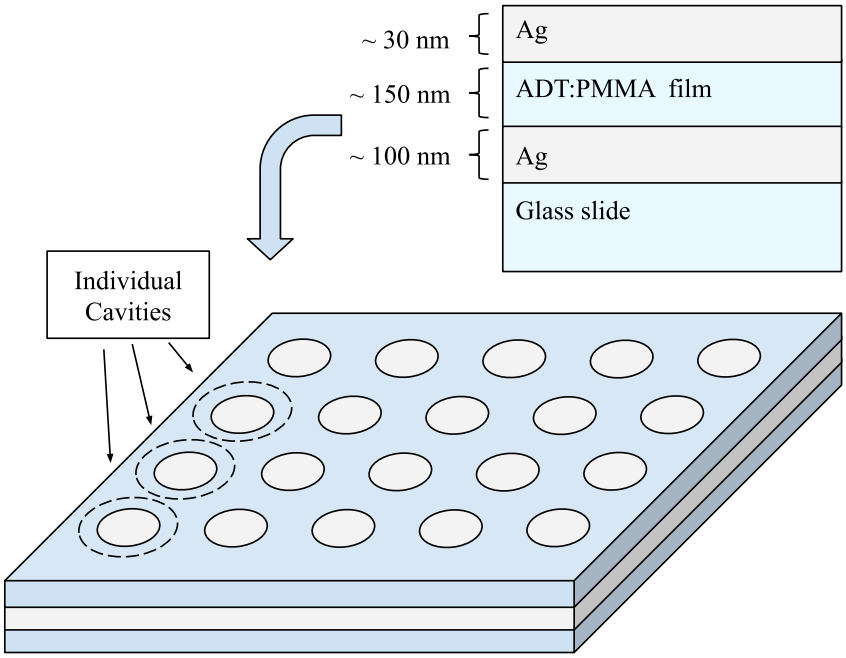

Figure 4 A "Cavity" composed of an array of individual cavities with the same thickness and ADT concentration. The Fabry-Perot microcavities we fabricated for this experiment are composed of a glass slide foundation with sequential deposits of a strong silver mirror, ADT:PMMA film, and a circular partially transparent silver mirror cap.

Each circular mirror cap represents an individual cavity, but because every cavity on a given slide has the same (approximate) thickness and ADT concentration, the entire slide is referred to as one cavity (e.g. Cavity 1C). The individual caps have no designation. The cavity naming convention is batch number followed by arbitrary index. Slides 1A, 1B, and 1C were all part of a single long slide during silver deposition and scored and separated afterwards. Then the individual slides were spun cast with different solutions. Only cavities 1B, 1C, 6A, and 6B were used in the research detailed in this paper. Table 2 can be found in the results section (pg 22) showing cavity parameters.

2.2 PHOTOLUMINESCENCE PL AND ABSORPTION MEASUREMENTS

To excite the samples, we wanted to use our 532 nm laser to take advantage of its variable laser power, but ADT cavity emission ranges from ~ 527 nm to ~590 nm and the cutoff filter we use in our setup interrupts our data. A 355 nm laser was used for all data collection in this paper.

I measured the PL and absorption on 4 cavity sites and 2 open sites for each of the 6 slides in the batch, each containing 0.4 M PMMA and varying concentrations of ADT. The laser penetrated the sample from below and pass through to the microscope objective. Both the laser and the microscope detection were fixed normal to the cavity for these measurements.

PL curves were taken with SpectraSuite (1.6.0_11) using an Ocean Optics USB2000 spectrometer. A dark spectrum was captured and subtracted from each measurement to remove ambient light noise. The laser used was a DualChip NanoLaser (class 4) of pulsed 355 nm light.

2.3 ANGLE RESOLVED PHOTOLUMINESCENCE (ARPL)

The ARPL measurements were done in two sets, the first one being done with a faulty understanding of the process laid out in the professional literature, and the second one with a corrected methodology.

Set one was collected in the same way as the measurements in section 2.2, except that the laser's angle of incidence was varied from -40° to +40° from normal at increments of 5°.

Set two was collected in the same way as set one, except that the laser's angle of incidence was fixed at normal and the angle of detection was varied instead (Figure 5). This set was completed twice for each sample, once at p-polarization, and once at s-polarization.

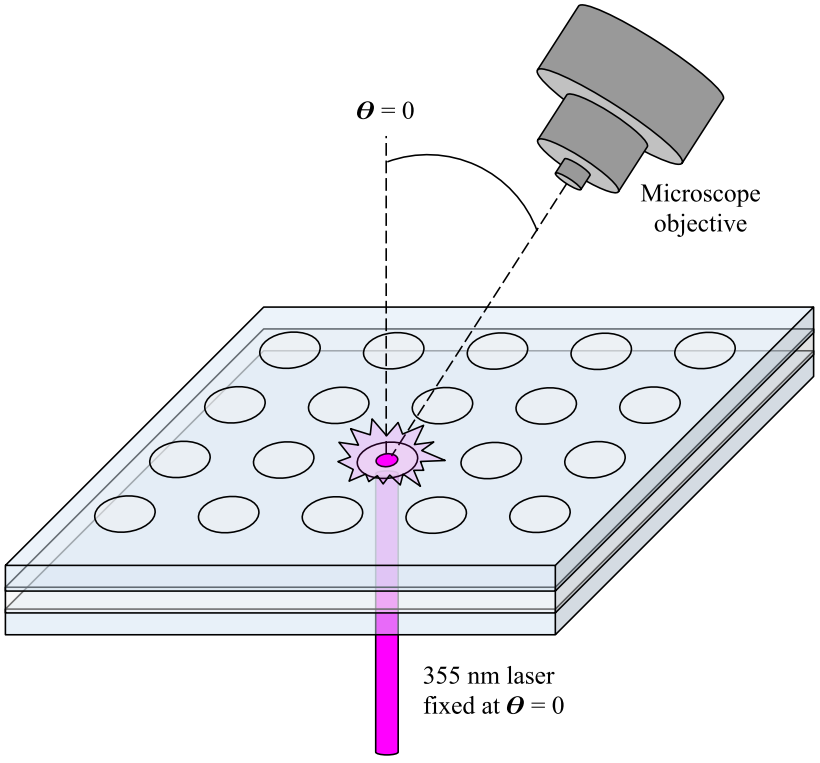

Figure 5 The second set of ARPL measurements kept the laser's angle of incidence fixed at normal and varied the angle of detection. Great care was taken to ensure that the laser and objective were focused on the same microcavity spot while varying angles.

3 RESULTS

3.1 CAVITY DESIGN

The E-beam deposited silver layers in the microcavities turned out smooth and highly reflective with little to no physical imperfections. While the goal was to deposit a silver foundation layer of 100 nm for nearly complete reflectivity and a cap layer of 30 nm for partial reflectivity, the E-beam deposition process was imprecise in its thickness distribution. Three or four slides could be lined up in the deposition chamber and coated at once, but the slides toward the center received a thicker coat of silver than the outmost slides. This produced a noticeable difference in reflectivity across the sample set but did not seem to impact data collection in any significant way. We decided that it was not necessary to precisely confirm these silver thicknesses and their differences in reflectivity were ignored.

By adjusting PMMA concentration and spin cast RPMs, we designed a process to produce a microcavity of just the right thickness to contain a standing wave photon whose energy is roughly equal to the exciton energy ~2.37 eV. The relation between film thickness and PMMA concentration was 34.75 nm/mM for trial one and 47.5 nm/mM for trial two using the same spin speeds, but different stock solutions made by myself and Van Schenck respectively.

The film thicknesses of the pure PMMA on silver mentioned in section 2.1 were measured using ellipsometry giving the values in Figure 6. The 1 M data point was considered an outlier and removed.

Table 1

Concentration (M)	Thickness (nm)
0	0
0.1	35 ± 5
0.3	104 ± 3
0.4	139 ± 3
0.5	190 ± 3
0.7	266 ± 5
1	446 ± 5

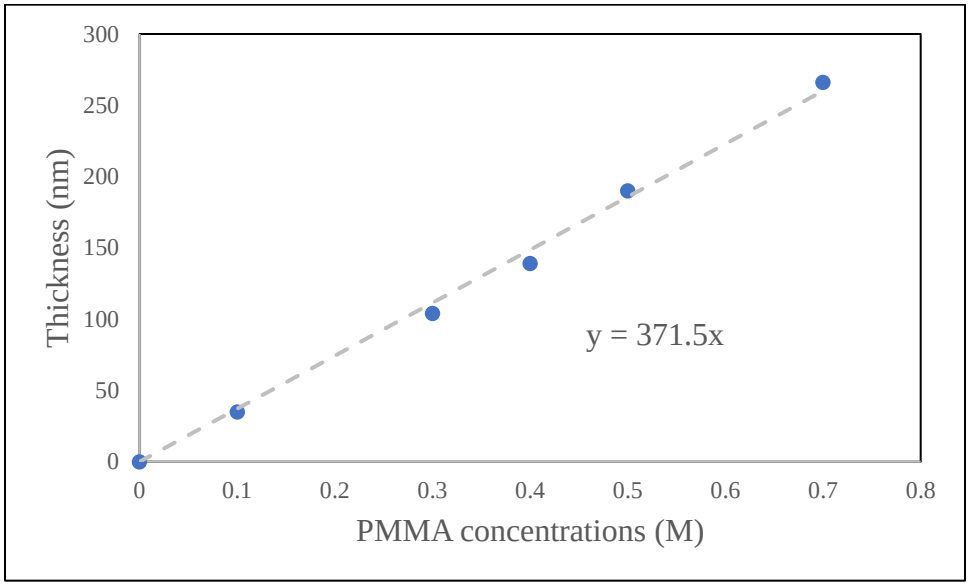

Figure 6 Film thicknesses of pure PMMA spun cast onto silver. Measurements were done with ellipsometry. The data suggests that for every 0.1 M of PMMA, the film thickness increases by ~37 nm.

Ellipsometry measurements yielded an effective index of refraction n = 2.2 for p-polarized light, and n = 1.55 for s-polarized.

3.2 MEASUREMENTS

I measured the PL and absorption on 4 cavity sites and 2 open sites for each of the 6 slides in the batch, each containing 0.4 M PMMA and varying concentrations of ADT. Both the laser and the microscope detection were fixed normal to the cavity for these measurements. As an

example, Figure 7 shows the photoluminescence and absorption data collected from slide 6B, which has a film thickness of 142.6 nm and an average distance of 3 nm between ADT molecules.

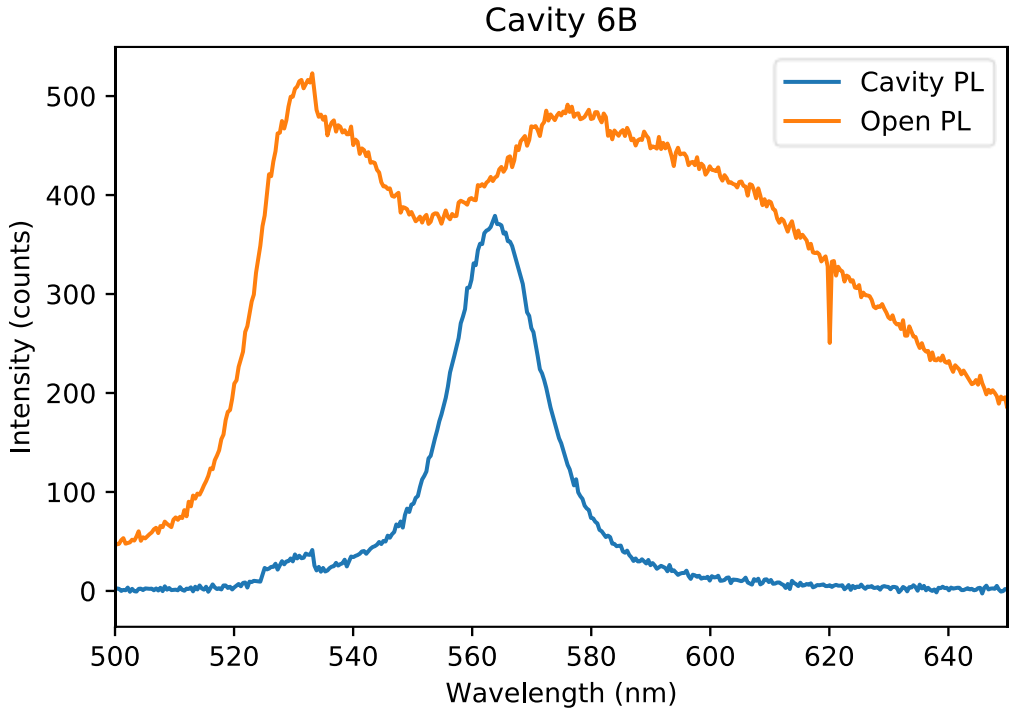

Figure 7 Cavity 6B has a film thickness of 142.6 nm and an average distance of 3 nm between molecules of ADT. The figure shows PL data taken from two sites on the same sample. The (Orange) curve is from an exposed ADT:PMMA film outside of the cavity and is consistent with the known PL behavior of ADT. The (Blue) PL curve is from a microcavity containing the same ADT:PMMA film. This curve shows that the cavity selectively emits light that has a wavelength compatible with the cavity's resonance.

The orange curve, labeled "Open PL", shows the intensity and wavelength of light emitted from the exposed ADT:PMMA film (outside the cavity) while being excited by a 355 nm laser and is consistent with known ADT photoluminescent behavior. The blue curve, labeled "Cavity PL," that peaks at a wavelength of 565 nm was gathered from one of the silver capped microcavities on the same glass slide.

These microcavities showed visible imperfections when viewed under the microscope (Figure 8).

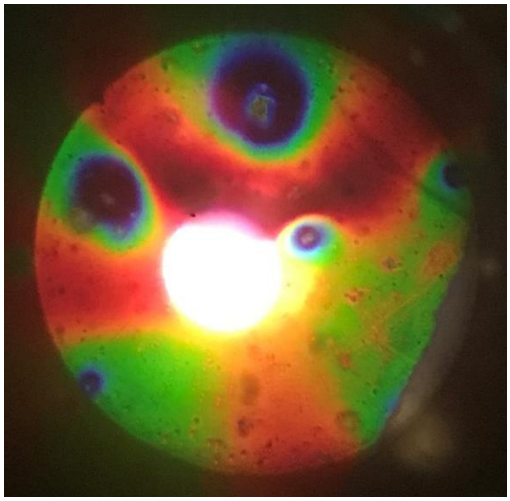

Figure 8 Microscope image of a microcavity containing PMMA and incomplete dissolution of ADT backlit by white light.

The solution used to make these cavities was not sonicated long enough and some ADT remained undissolved which lead to clumps in the thin film causing variances in film thickness. The sites measured were selected to avoid problem spots such as these as much as possible. The data curves seemed to come out fairly clean despite these imperfections.

The varied laser angle ARPL measurements for set one discussed in methods section 2.3 yielded the curves seen in Figure 9. While this data cannot tell us anything about the polaritonic state within the sample, it can be used as a check of our understanding. The energy of the emitted photons (those captured, anyway) did not change with the laser's angle of incidence.

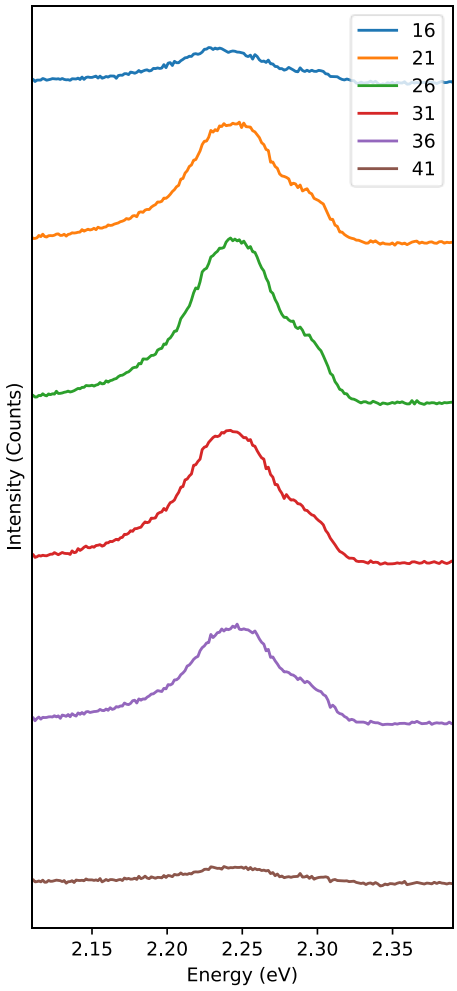

Figure 9 Data from set one ARPL method using Cavity 6A. During this data collection, the angle of incidence of the laser was varied instead of the angle of detection. The emission intensity changes with angle of incidence but the photon energy does not.

The primary method ARPL data from set two is represented in Figure 10, which shows the energy of the photons as they resonate and are emitted from the microcavity at varying angles of detection. This data was used with Equation (8) to generate the dispersion relation to

determine the Rabi splitting energy (2V) when the energies of the cavity photon and exciton are equal.

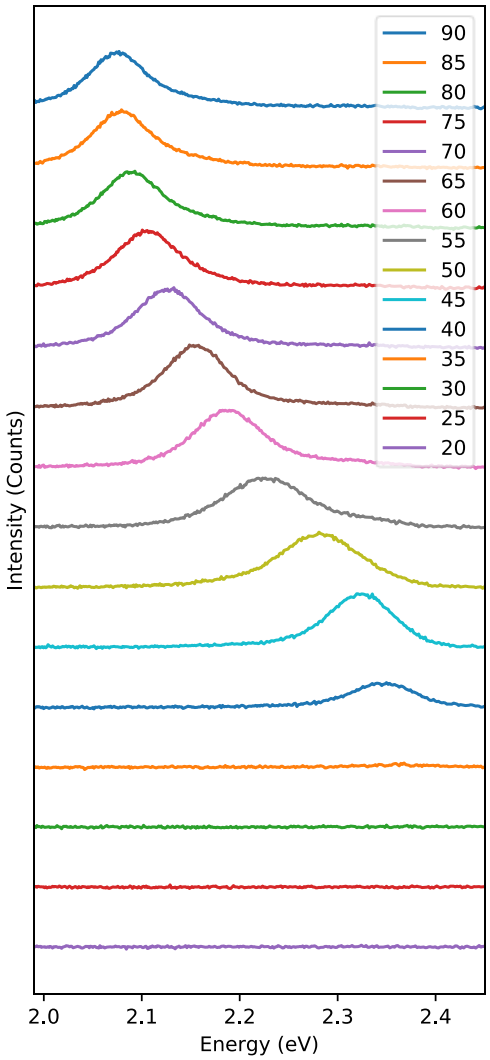

Figure 10 Data from corrected ARPL method using Cavity 1C. During this data collection, the angle of the laser was fixed at normal (s-polarized) and the angle of the detecting microscope objective (upper right column) was varied. The emission peak migrates with angle of detection in accordance with Equation (8).

The photon energies corresponding to the peaks in Figure 10 are plotted against the angle of detection in Figure 11. These curves represent the lower polariton energy of the coupled cavity system, like the lower polariton energy shown in Figure 2.

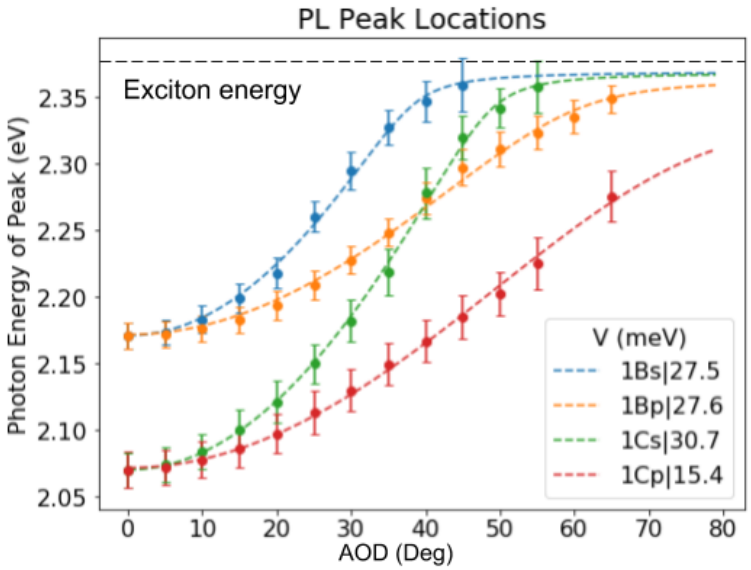

Figure 11 This plot tracks the peak energy of the ARPL curve over the angle of detection. Each curve in this plot represents the migration of peak energy in an entire data set, like that presented in Figure 10. This information is used to calculate V (half of the Rabi splitting energy) using Equation (8). Each point is a peak location and the dotted line is a fit. The legend gives the calculated values of V in meV for Cavity 1B (s- and p-polarization), and Cavity 1C (s- and p-polarization). The energies of s- and p-polarization data sets differ because the cavity's effective index of refraction varies with polarization due to the polarizability of the cavity.

Table 2

Cavity	PMMA	Spin cast speed	d	Thickness	Rabi energy (2V)
1B (s-polarization)	0.4 M	1780 RPM	5 nm	147 nm	55 meV
1B (p-polarization)					55 meV
1C (s-polarization)	0.4 M	1860 RPM	4 nm	149 nm	61 meV
1C (p-polarization)					31 meV
6A	0.4 M	1940 RPM	3.5 nm	138 nm	Untested
6B	0.4 M	2090 RPM	3 nm	143 nm	Untested

4 DISCUSSION

The Cavity 6B PL curve in Figure 7 is significant because it shows that the light emission is being limited to a wavelength that is consistent with the resonance of the cavity. An emission wavelength of 565 nm indicates a wavelength of ~379 nm inside the cavity due to the wavelength relation,

$$\lambda_{\mathrm{PMMA}} = \frac{\lambda_0}{n_{PMMA}} = 379\ \mathrm{nm}, \tag{4}$$

where λ_{PMMA} and n_{PMMA} are the wavelength and refractive index respectively inside the cavity, and λ_0 is the wavelength in vacuum (approximately equal in air), which suggests the half wavelength contained inside the cavity is ~189 nm. Since this value is at odds with the cavity thickness from ellipsometry (142.6 nm) and the sample was excited with unpolarized light, other contributions to the effective index of refraction seem to be at play.

This fixed angle experiment was only intended to provide preliminary data to inform future methods of cavity fabrication by showing that the cavity is selecting an optical mode as expected.

The ARPL measurements and Rabi energy calculations were successful in showing polaritonic behavior in the ADT molecule. Although the Rabi energies we found are small (at most, 61.4 meV), this is to be expected in very dilute systems and the prospective energies in crystalline ADT systems is promising.

Because our data collection consisted only of emission spectra, the lower polariton branch is all we have access to. This is due to the way in which the energy of the excitation settles to its lowest manifold state before it emits as light because some energy is lost to non-emitting modes, such as vibration.

5 CONCLUSION

Exciton polaritons show promise in the development of future technologies, such as polariton lasers, which have low lasing thresholds, optical communication lines, solid state lighting, and medicine. The goal of this work was to design and fabricate a Fabry-Perot microcavity system in which to produce exciton polaritons, and to show evidence of polariton occurrence by determining the Rabi splitting energy with angle resolved photoluminescence. This work was motivated by the prospect of using organic semiconductors in polaritonics research to take advantage of their large exciton binding energies, ease and flexibility of production, and their ability to host polaritons at room temperature.

The microcavity fabrication and ARPL measurements were successful and lead to insights, such as cavity thickness dependencies and coupling strengths, which will inform a more precise fabrication and measurement process in the future. We conclude that exciton polaritons were indeed produced in our microcavities as evident by strong coupling of excitons and cavity photons, and that coupling strength is dependent, in part, on ADT concentration, and polarization and resonance angle inside the cavity. Future work may include a larger set of measurements on a wide range of ADT concentrations for statistical integrity, fabrication and reflectivity measurements of cavities containing ADT in crystal form, testing the effects of crystal stacking structure on Rabi energy, as well as characterization of electrical properties of exciton polaritons in dilute ADT films and crystals.

Bibliography

[1] D. Sanvitto, S. Kena-Cohen, “The road towards polaritonic devices,” *Nature Materials*, vol. 15, pp. 1061-1073, 2016

[2] A. V. Kavokin, J.J. Baumberg, G. Malpuech, F.P. Laussy, “Microcavities,” (textbook) Oxford University Press, 2017

[3] A. Graf, L. Tropf, J. Zaumseil, M. C. Gather, in Handbook of Organic Materials for Electronic and Photonic Devices, Elsevier, pp. 281–307, 2019

[4] P. Torma and W. L. Barnes, “Strong coupling between surface plasmon polaritons and emitters: a review,” *Reports on Progress in Physics*, vol. 78, pp. 1-34, 2015

[5] R. J. Holmes, S. R. Forrest, “Strong exciton-photon coupling in organic materials,” *Organic Electronics*, vol. 8, pp. 77-93, 2007